

Report 2844

Construction and Operation of a Hot-Corrosion Test Facility

AD 684440

# NAVAL SHIP RESEARCH AND DEVELOPMENT CENTER

Washington, D.C. 20007



NAVAL SHIP RESEARCH AND DEVELOPMENT LABORATORY  
Annapolis, Maryland 21402

## CONSTRUCTION AND OPERATION OF A HOT-CORROSION TEST FACILITY

By  
Harvey von E. Doering and Paul A. Bergman

This document has been approved for public release and  
sale; its distribution is unlimited.

DDC  
MAR 27 1969

MATERIALS LABORATORY  
RESEARCH AND DEVELOPMENT REPORT

March 1969

Report 2844

CLEARING HOUSE

The Naval Ship Research and Development Center is a U.S. Navy center for laboratory effort directed at achieving improved sea and air vehicles. It was formed in March 1967 by merging the David Taylor Model Basin at Carderock, Maryland and the Marine Engineering Laboratory at Annapolis, Maryland.

Naval Ship Research and Development Center  
Washington, D.C. 20007

ACCESSION	
GTST	
DOC	
DATE	
BY	
OR	
DIST.	

CONSTRUCTION AND OPERATION  
OF A HOT-CORROSION TEST FACILITY

By  
Harvey von E. Doering<sup>1</sup> and Paul A. Bergman<sup>2</sup>

---

<sup>1</sup>  
Senior Project Engineer, High Temperature Alloys, Annapolis Division, Naval Ship  
Research and Development Center, Annapolis, Maryland.

<sup>2</sup>  
Senior Engineer, Thomson Laboratory, Aircraft Engine Group, General Electric  
Company, Lynn, Massachusetts.

### ABSTRACT

An apparatus, the burner rig, used to evaluate materials for use in gas-turbine engines operating in a marine environment, is described. Testing procedures are outlined, and results are discussed in relation to gas-turbine engine tests.

The rig operates by the combustion of diesel oil or jet fuels. Injected seawater and the products of combustion pass over as many as 48 test specimens. Although the rig operates at atmospheric pressure and low velocities, it can generate a test environment that results in hot corrosion as found in actual engines, is economical to construct, and can operate unattended for long periods of time over a wide range of closely controlled conditions.

Data are shown for some commercial nickel- and cobalt-base alloys tested at 200 parts per million (ppm) sea salt/100 hours and 5 ppm sea salt/1000 hours. Comparisons are made between photomicrographs of the corroded zones of engine parts and specimens tested at 0.5, 5.0, and 200 ppm sea salt. Empirically, 200 ppm sea salt is too heavily oriented toward sulfidizing effects, and oxidation does not play a dominant enough role in the net corrosion process. It appears that 1000 hours with 0.5 ppm sea salt represent realistic test conditions.

#### ADMINISTRATIVE INFORMATION

This report constitutes Fiscal Year 1969, Milestone 1, on page 98 of the October 1968 Program Summary of the Annapolis Division, Naval Ship Research and Development Center. This work was supported by Assignment 1-815-122-A, Subproject S-F013-06-04, Task 12725, on Gas Turbine Materials, Corrosion.

The report was presented as a technical paper at the annual meeting of ASTM in June 1968.

#### ACKNOWLEDGMENT

The authors are grateful to Mr. Robert Bartocci for engineering and design contributions leading to the successful operation of the equipment.

## TABLE OF CONTENTS

	<u>Page</u>
<b>ABSTRACT</b>	iii
<b>ADMINISTRATIVE INFORMATION</b>	iv
<b>INTRODUCTION</b>	1
<b>EQUIPMENT</b>	2
<b>BASIC DESIGN</b>	2
<b>FURNACE</b>	3
Temperature	3
Fuel	3
Air and Fuel Mixture	4
Sea Salt	4
<b>THERMAL CYCLING</b>	4
Controls	4
Manpower	5
<b>TEST SPECIMENS AND EVALUATION</b>	5
<b>SPECIMENS</b>	5
<b>SPECIMEN EVALUATION</b>	5
<b>TESTING PROCEDURES AND RESULTS</b>	6
<b>SUMMARY</b>	8
<b>LIST OF FIGURES</b>	
Figure 1 Photograph; Severe Hot Corrosion of AMS5391A	
Figure 2 Photograph; Burner Rig and Associated Equipment	
Figure 3 Schematic Cross Section of Burner Rig	
Figure 4 Drawing; Expanded View of Burner Rig Showing Placement of Essential Components (2 pages)	
Figure 5 Fuel Nozzle Assembly	
Figure 6 Sea-Water Atomizer	
Figure 7 Schematic Diagram of Plumbing for Fuel, Sea-Water Solution, and Air	
Figure 8 Electric Circuit Diagram	
Figure 9 Method of Measuring Hot-Corrosion Attack	
Figure 10 Photomicrograph; Cross-Section Area of the Leading Edge of a Corroded AMS5391A Nozzle Vane	
Figure 11 Photomicrograph; AMS5391A Nozzle Vane Illustrating the Small Grey Globular Phase at the Interface of the Oxides and Base Matrix	
Figure 12 Photomicrograph; Cross-Section Area of an AMS5391A Specimen Tested at 1550° F for 1000 Hours with 0.5 PPM Sea Salt	
Figure 13 Photomicrograph; Cross-Section Area of an AMS5391A Specimen Tested at 1600° F for 1000 Hours with 5 PPM Sea Salt	
Figure 14 Photomicrographs; Specimen Tested at High Sea-Salt Concentrations	
Figure 15 Temperature Range of Hot Corrosion For Two Test Conditions	
<b>APPENDIXES</b>	
Appendix A	
<b>DISTRIBUTION LIST</b>	

# NAVAL SHIP RESEARCH AND DEVELOPMENT LABORATORY

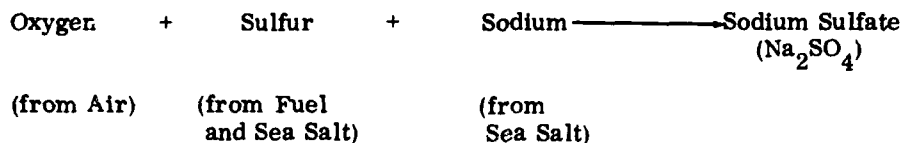
## CONSTRUCTION AND OPERATION OF A HOT-CORROSION TEST FACILITY

By  
Harvey von E. Doering and Paul A. Bergman

### INTRODUCTION

The ingestion of sea salt by gas-turbine engines operating in marine environments can lead to corrosion of hot section components, particularly turbine vanes (nozzles) and blades (buckets). A typical corroded part from a commercial test engine, illustrated in Figure 1, and many other cases of similar severe corrosion have been documented in the open literature.<sup>1, 2</sup> This attack has been identified as sulfidation, which is a form of hot corrosion.

Molten sodium sulfate is the principal agent in causing hot corrosion and is formed as follows:



Excess oxygen and sulfur are always present during engine operation; hence, the introduction of sodium in the form of sea salt can cause hot corrosion. Severe hot corrosion occurs only in a certain temperature range in which the sulfate deposits on parts in a molten state.<sup>3</sup> The existence of such a temperature range has also been demonstrated by Walters.<sup>4</sup> Below the melting point of the sulfate or above the temperature at which it is vaporized, the sodium sulfate is relatively innocuous.<sup>5</sup> These temperatures are dependent on conditions of the environment. For example, the melting point of sodium sulfate is effectively lowered due to the formation of a eutectic with sodium chloride.<sup>1</sup> Also, DeCrescente, et al,<sup>5</sup> have described the relationship between the dew point of sodium sulfate and the pressure and amount of sodium chloride (assuming complete conversion of sodium chloride to sodium sulfate).

In the beginning, crucible tests which require either complete or partial immersion of the samples in the corrodant contained within a crucible were the predominant type. Although such tests do not duplicate engine environments well, they are still quite useful in studying the mechanism of hot corrosion under precisely controlled conditions. Recent, more sophisticated, tests are run in rigs that burn liquid fuels or natural gas to generate simulated turbine-exhaust gases. Sea salt is added to simulate operation in a marine environment. Such burner rig tests are more appropriate for evaluating alloys and coatings for engine applications.

<sup>1</sup>Superscripts refer to similarly numbered entries in Appendix A.

Although the ultimate selection of materials must be based on testing in gas-turbine engines, such tests are time consuming and expensive. Thus, the laboratory burner rig is necessary as a means of studying the hot-corrosion problem and screening various materials under closely controlled conditions. These conditions simulate but do not necessarily duplicate the gas-turbine environment. One of these burner rigs, described herein, operates on diesel oil or high distillate fuels (JP4, JP5, etc) at relatively low pressure and velocity. The construction and operation of the burner rig are described in detail; testing procedures are discussed and some correlations to engine experience are drawn.

## EQUIPMENT

### BASIC DESIGN

A photograph, a schematic cross section, and an expanded view of the components of the burner rig appear as Figures 2, 3, and 4, respectively. In operation, fuel is metered through a hypodermic needle in the fuel nozzle (Figure 5 and C of Figure 4), atomized and burned in the forward zone of a 2 3/8-inch-diameter ceramic tube, referred to as the combustion tube (H of Figure 4). Sea salt or other soluble contaminants are atomized (Figure 6 and D of Figure 4) and injected into the combustion area. The gases and sea salt are thoroughly mixed by the swirl action of air entering through tangential slots in the combustion tube. This design precludes stagnation or stratification of the combustion gases. Downstream, the test specimens are exposed to the products of combustion and sea salt (or other contaminants). A test specimen fixture, rotating at 20 rpm (P of Figure 4) assures equal exposure of all test specimens.

Temperatures are attained by the combustion of the fuel supplemented by heat from resistance wound heating elements (J and N of Figure 4) which surround the combustion tubes and the test chamber. The heaters reduce temperature gradients and permit operation at a range of temperatures between 1500° and 2100° F.\* Air/fuel ratios range from 15 to 1 (approximately stoichiometric conditions) through at least 60 to 1. Within certain limits, temperature changes can be made without changing combustion conditions. Conversely, constant temperatures can be maintained while varying combustion conditions. Flame impingement on the specimens is normally avoided. On the other hand, fuel-rich conditions or flame impingement is obtainable as a special test condition. The heaters also provide a safety feature since they maintain high temperature throughout the rig and cause instantaneous combustion of the fuel.

Figure 7 is a schematic diagram of the plumbing arrangement for supplying air, fuel, and sea salt to the burner rig. Both fuel and salt solution are fed from supply tanks through positive displacement gear pumps to flowmeters, filters, and relief valves to the combustion zone.

---

\*Abbreviations used in this text are from the GPO Style Manual, 1967, unless otherwise noted.

The electrical portion of the equipment, Figure 8, is primarily concerned with temperature control through the heating elements and with safety interlocks. There are sufficient safety controls (detailed in succeeding sections) that, in combination with operation at relatively low pressure and low fuel flow, the burner rig may be placed in a regular laboratory area with no heavy test-cell-type construction (Figure 2.)

## FURNACE

The furnace is constructed of a stainless steel shell (A of Figure 4) and filled with a refractory cement. The furnace is designed to be split in half, allowing easy disassembly for maintenance work necessitated by the destructive nature of the molten salts. The mating surfaces, when closed, are best sealed with asbestos cloth. At the specimen zone, the top half of the furnace is hinged so that it may be opened easily for adding the test specimens after operation at steady-state conditions is achieved. This avoids exposing the specimens to the fuel-rich conditions at start-up times and ensures that specimens reach test temperatures quickly.

The heating elements are constructed with coiled resistance wire which is cast within a readily castable refractory. All of the heaters are shielded from the combustion gases and salts with alumina tubes or muffles and cemented in place with an alumina-base cement; alumina is considered an inert material. This protects the heaters and prevents contamination from the test environment of the refractory in which the heaters are cast. The combustion tubes may be purchased as a commercial shelf item.

Most of the heating elements are wired in parallel so that a failure of one of them does not necessitate a shutdown. Also the exposed lead wires are double wound so that they will remain cooler and less susceptible to corrosion and oxidation during operation. The heaters have demonstrated at least a 4000-hour life. Replacement of the elements is a large effort, since they are cemented in place; it takes about 30 man-hours.

## Temperature

The heating elements control the temperature within  $\pm 15^\circ \text{F}$  through a thermocouple at the center of the rotating specimen fixture. During testing, the temperature is monitored with optical pyrometer readings of the rotating specimens through the exhaust tube. Periodic checks are made with a two-color pyrometer. This temperature control is based on an initial correlation between the optical pyrometer, the stationary thermocoupled specimens, the two-color pyrometer, and the hardness of age hardening alloys.

## Fuel

Diesel and high distillate fuels (JP4 and JP5) have been used and presumably other similar liquid fuels are possible. Ditertiary butyl disulfide can be added to diesel fuel to increase the sulfur concentration, if desired. A positive displacement gear pump is used for a low, steady, and accurate fuel flow generally in the range of 8 to 10 cc per min or about 3 to 4 gallons in 24 hours. A flowmeter calibrated by measuring the time it takes to fill a graduate at the fuel nozzle indicates flow rate. In addition, the level of fuel in the tank is measured every day for a calculation of total fuel used.

The fuel is atomized into a fine dispersion by high-pressure air and introduced into the combustion end of the furnace. The combination of a fine spray of fuel, excess air, and high temperatures achieves instantaneous combustion.

#### Air and Fuel Mixture

Filtered compressed air is reduced sufficiently in pressure by a pressure regulator to eliminate the usual line-pressure fluctuations. For example, a line pressure of 95 psi is reduced to 75 psi for rig consumption, but other air pressures could be used just as well. The total air used is monitored by a flowmeter, corrected for pressure, to control air/fuel ratios and salt concentrations. Beyond the flowmeter, the air is divided into three lines leading to the fuel nozzle, salt nozzle, and the tangential slots of the combustion tube. Each of these three air lines is controlled with pressure regulators. The air entering the tangential slots of the combustion tube is preheated by the stainless steel aligning tube (G of Figure 4) which is surrounded by two semicylindrical resistance heaters.

Most tests have been conducted at 30 to 1 air/fuel ratios. A 60 to 1 ratio is possible, but the maximum test temperature under these conditions is limited to about 1900° F. A fuel-rich or reducing condition can be obtained by reducing the airflow. In this case, a "soft" yellow flame burns throughout the rig exposing the specimens to some carbon, carbon monoxide, and hydrogen.

#### Sea Salt

Sea salt or other contaminants are introduced in the desired amount in a water solution. The solutions are pumped, metered, and atomized in about the same manner as the fuel. The fine spray is injected into the combustion zone to duplicate high-temperature reactions occurring in gas turbines. The ceramic tubes and absence of metallic parts permit the use of the highly active molten salts in the combustion zone of the rig.

#### THERMAL CYCLING

Automatic thermal cycling has not been incorporated into the design of the rig; however, manual cycling can be accomplished easily. In less than 30 seconds, the fixture with the specimens can be removed from the rig and placed in a vise for cooling to room temperature with an air blast. This is also an opportune time to make visual ratings of the specimens.

#### Controls

Two separate thermocouples are used. The control thermocouple is positioned in the center of the rotating specimens through Area M of Figure 4 and is connected to a recorder controller which operates a silicon controlled rectifier or saturable core reactor of about 50 amperes at 110-volt capacity. Microswitches in the temperature recorder are set to shut down the test stand for temperature variations in excess of  $\pm 25^\circ$  F beyond the normal temperature cycling range.

The other thermocouple is solely a safety feature. It is positioned in the combustion area between the steel alignment tube and the combustion tube through Area K of Figure 4. The thermocouple is connected to a double set point on-off controller.

If a flame-out or improper combustion occurs, the temperature will quickly drop below the preset lower limit and the controller will shut off the rig. Also, a rise in temperature above the preset limit, perhaps due to air stoppage or excess fuel flow, will similarly affect shutdown. Both thermocouple controls have break and short protection. In addition, a power failure, even a momentary one, will shut the rig off, and a manual procedure is needed for restart.

Other safety features include a relief valve on the fuel tank. A bypass system in the fuel line is constructed so that if the fuel nozzle becomes clogged, the fuel will be bypassed back to the supply tank. Finally, a heat detector head, set for a rise of 10° F per minute, is placed under each rig and it is connected to a fire alarm system. These controls permit unattended operation of the rig.

### Manpower

In operation, one man can operate four rigs for long-time tests (500 to 1000 hours) and about 2 1/2 rigs for the short-time tests (50 to 100 hours). The lower efficiency for the latter tests is due to the increased time for preparing new setups, cleaning, and attending equipment malfunctions caused by clogging and corrosion of equipment from the higher salt concentrations used in such tests. Also, the long-time tests can operate around-the-clock 7 days a week, whereas the short-time tests may have to be shut down because of scheduling on a one-shift basis.

## TEST SPECIMENS AND EVALUATION

### SPECIMENS

Eight specimens of 1/2-inch diameter x 3-inch length are tested at one time. Larger specimens, even engine parts or segments thereof, may also be tested. For long-time tests, it is economically advisable to test as many specimens as possible in each run. Therefore, up to 48 smaller specimens (1/8-inch diameter x 1 1/2-inch length) can be tested simultaneously.

Specimen fixtures are generally made of AMS5536D (composition in Table 1) which has a relatively good resistance to hot corrosion. They can be additionally protected with an aluminum diffusion coating.

### SPECIMEN EVALUATION

Metallographic measurements are used to determine the degree of attack. In this method, each of two transverse cross-section areas are measured for hot-corrosion effects along two diameters approximately 90 degrees apart. Values are reported as surface loss and maximum penetration, as illustrated in Figure 9. Surface loss is the effective metal loss by massive oxidation and sulfidation; it does not account for subsurface effects such as intergranular attack. For each specimen, all measurements are averaged together for one value. Surface losses are pertinent for low stress applications like turbine vanes. These parts can maintain functional integrity as long as they hold their shape. Maximum penetration is a measurement which includes surface loss plus the depth of all oxides and sulfides; these may be scattered or in local concentrations such as grain boundaries. Only the greatest depth value is reported as the maximum penetration. These measurements are most relevant to high stress applications such as turbine blades. Subsurface attack in local areas may also promote failures through fatigue or thermal fatigue.

Table 1  
Nominal Composition of Alloys

Alloys	Composition											
	Ni	Cr	Co	Fe	Mo	W	Al	Ti	B	Z	C	Others
5536D	Bal	21.0	1.8	19.0	8.7	0.5					0.12	
5384	Bal	18.8	19.4	0.2	4.2		3.0	3.0	0.005		0.08	
5391A	Bal	13.0	1.0 <sup>(1)</sup>	2.5 <sup>(1)</sup>	4.5		6.0	0.8	0.01	0.10	0.14	2.3 Cb + Ta
5397	Bal	10.0	15.0	1.0 <sup>(1)</sup>	3.0		5.5	5.0	0.2	0.06	0.18	0.9V
PA1 <sup>(2)</sup>	Bal	15.0	26.0	1.0 <sup>(1)</sup>	4.5		4.4	2.3		0.015	0.08	
PA2 <sup>(2)</sup>	Bal	11.0	14.5	0.5 <sup>(1)</sup>	6.5	1.5	5.4	2.5		0.015	0.07	0.4 Cb + Ta
PA3 <sup>(2)</sup>	Bal	8.8	10.2	0.3		12.3	4.9	1.8		0.015	0.14	1.2 Cb
5382D	10.5	25.5	Bal	2.0 <sup>(1)</sup>		7.5					0.45	
5759C	10.0	21.0	Bal	3.0		15.0					0.10	

<sup>1</sup>Maximum

<sup>2</sup>Proprietary Alloy

Bal-Balance

Round specimens can be measured accurately by the metallographic technique across any diameter, which is an important consideration since an uneven attack frequently occurs. Wedge, airfoil, or other unevenly shaped specimens are generally too difficult to analyze except when using the weight change method for measuring the degree of corrosion. However, a weight change, per se, is not always adequate although it allows for more continuous measurements during exposure. Three of the limitations of the weight method are (1) it lacks the registering of subsurface attack, like intergranular attack, which at times is quite deep; (2) deep localized corrosion (e. g., pitting) is averaged over the weight of the entire specimen and, thus, the extent of the attack is minimized; and (3) weight gains due to oxygen or sulfur absorption would interfere with weight loss measurements.

#### TESTING PROCEDURES AND RESULTS

It is relevant to conduct laboratory burner rig tests under conditions that are realistic compared to engine environments. Two of the most important testing variables for consideration are the sea-salt concentrations and test time. Unfortunately, no quantitative data are known to exist on amounts of sea salt reaching the hot section turbine components. To obtain enough corrosion in a reasonable length of time to be able to make distinctions between various alloys, laboratory tests need to be conducted at higher sea-salt concentrations than occur in an engine. Also, to duplicate the total sea salt in the turbine area with conditions of high pressure and velocity, resulting in high mass flow of air, a higher ppm concentration of sea salt is needed in a burner rig operating at low pressure and velocity.

In particular, the higher sea-salt concentration in the laboratory test tends to compensate for its lower pressure in regard to approximating the dew point for condensation of sodium sulfate in an engine. After the appropriate testing parameters are chosen, they can be verified on an empirical basis by comparing test specimens to engine parts with regard to alloy behavior and morphology of attack.

The burner rig described herein has been used for testing at 0.5, 5.0, and 200 ppm sea salt, but mostly at the latter two concentrations. The lower salt tests are run for 500 and 1000 hours and the 200 ppm salt tests for 100 hours. Typical photomicrographs of the corroded zones of specimens from the burner rig tests and an engine part appear as Figures 10 through 14. The condition of the engine part is, in many respects, similar to that of many others reported in the open literature.<sup>1,2</sup> The engine part at low magnification in Figure 10 shows a deeply corroded area with a fine texture of oxides and remaining metal (depleted of alloying elements such as chromium, aluminum, and columbium) in the form of striations. At the interface of the oxides and base metal, there are small grey globular, chromium-rich sulfides which can be resolved only at relatively high magnification, as shown in Figure 11. Laboratory specimens tested at various salt concentrations may have comparable microstructures in selected areas compared to Figure 11, but only specimens tested at low salt concentrations also appear metallographically similar to the engine part on a gross basis, i.e., at low magnifications. A low-magnification photomicrograph of a specimen tested at 0.5 ppm sea salt (no thermal cycling) Figure 12, looks quite similar to the engine part in Figure 10 in regard to a fine texture and striations. At 5 ppm, some alloys appear somewhat similar as shown in Figure 13, but the texture of oxides and metal is coarser. Many alloys at 5 ppm sea salt, and especially at 200 ppm, have many large chromium-rich sulfides and even nickel sulfides, as shown in Figure 14. Thus, the higher sea-salt tests, especially those at 200 ppm, are heavily oriented toward sulfidation effects, as manifested by the formation of large sulfides. Empirically, oxidation does not appear to play a dominant role. On the other hand, the 0.5 ppm sea-salt test yields more of an oxidation oriented reaction as evidenced by the formation of more oxides and smaller (and fewer) sulfides. Therefore, it appears that a test condition of 0.5 ppm sea salt is realistic.

For tests of 5 ppm sea salt / 1000 hours, the temperature range of hot corrosion is about 1525° to 1800° F (the upper temperature limit is alloy dependent) as contrasted to about 1625° to 1900° F for 200 ppm sea salt/100-hour tests, as illustrated in Figure 15. Apparently, hot corrosion occurs at lower temperatures in the 5 ppm sea-salt test due to longer test times. Undoubtedly, corrosion would also occur at 200 ppm sea salt for periods of time longer than 100 hours. The upper temperature limit of corrosion is about 100° F higher for the 200 ppm sea-salt test due to a higher vaporization/condensation temperature of sodium sulfate at higher salt concentrations. Thus, care must be taken in designing and interpreting the "accelerated test." At low temperatures (e.g., 1600° F), hot corrosion may not occur because of the short test times. At high temperatures (e.g., 1800° to 1900° F) with high salt concentrations, a severe hot corrosion reaction may take place. However, only oxidation, or an "accelerated oxidation" aggravated by salt vapors, would occur for lower and more realistic sea-salt concentrations.

Even at a test temperature in which severe hot corrosion occurs for both the 5 and 200 ppm sea salt, some differences in alloy performance can be noted. Test results for the two salt concentrations at 1750° F are presented in Table 2 with the chemistries of the alloys in Table 1. For the 5 ppm/1000-hour test compared to the 200 ppm/100-hour test, one alloy (AMS 5759C) shows a decrease in attack, three alloys (AMS 5282D, AMS 5397, and PA1) are about the same, and four alloys (AMS 5384, AMS 5391A, PA1 and PA3) are attacked to a greater extent. Thus, the specific ranking of the alloys is dependent on the test conditions.

Table 2  
Burner Rig Test Results at 1750° F

200 PPM/100 Hours		5 PPM/1000 Hours	
Alloy	Attack mils <sup>1</sup>	Alloy	Attack mils <sup>1</sup>
5384	1.1/7.0	5382D	1.0/11.6
5382D	0.6/9.2	5759D	5.5/15.3
PA1	15.9/26.4	5384	8.8/31.7
5759D	10.7/27.8	PA1	31.5/51.8
PA3	14.4/44.5	5391A	59.0/77.1 <sup>2</sup>
5391A	56.6/65.8	5397	130 <sup>3</sup>
5397	130 <sup>3</sup>	PA3	130 <sup>3</sup>
PA2	130 <sup>3</sup>	PA2	130 <sup>3</sup>

<sup>1</sup>Results given as surface loss/maximum penetration expressed as losses in diameter as described in the section entitled Specimen Evaluation.

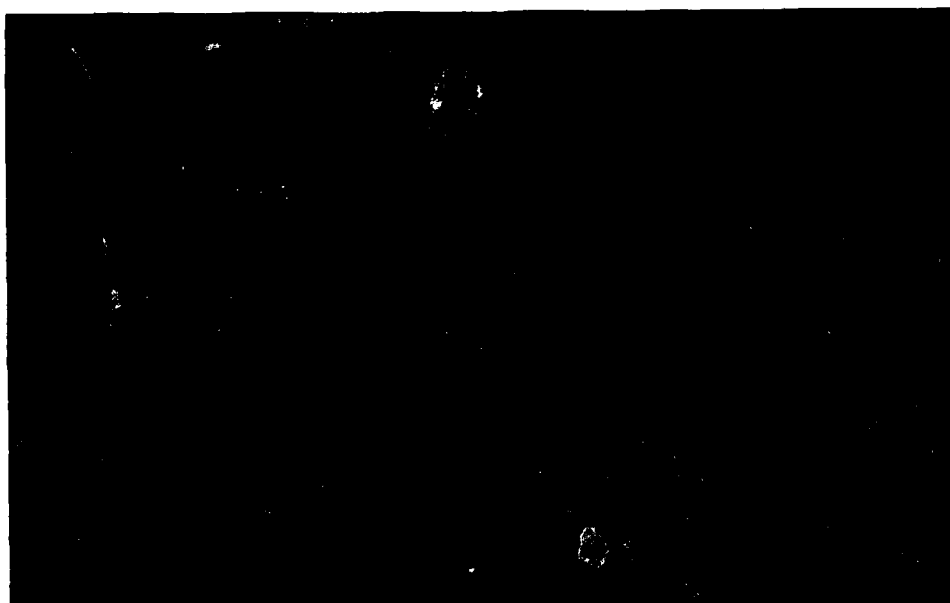
<sup>2</sup>At times, specimens of this alloy have been destroyed.

<sup>3</sup>Specimens destroyed.

#### SUMMARY

The burner rig described herein operates on diesel oil or high distillate fuels (JP4, JP5, etc) and generates an environment that results in hot corrosion as found in actual engines, although it operates at atmospheric pressure and low velocity. The main features of the rig are economy of construction and its capability of operating unattended for long periods of time and over a wide range of closely controlled test conditions. It appears that 1000 hours at 0.5 ppm sea salt represents realistic test conditions.

NAVAL SHIP RESEARCH AND DEVELOPMENT LABORATORY



Note: The leading edges of 1st stage nozzle vanes show considerable swelling and cracking.

Figure 1

Severe Hot Corrosion on AMS5391A

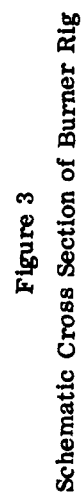
NAVAL SHIP RESEARCH AND DEVELOPMENT LABORATORY



Figure 2

Burner Rig and Associated Equipment

MATLAB 281



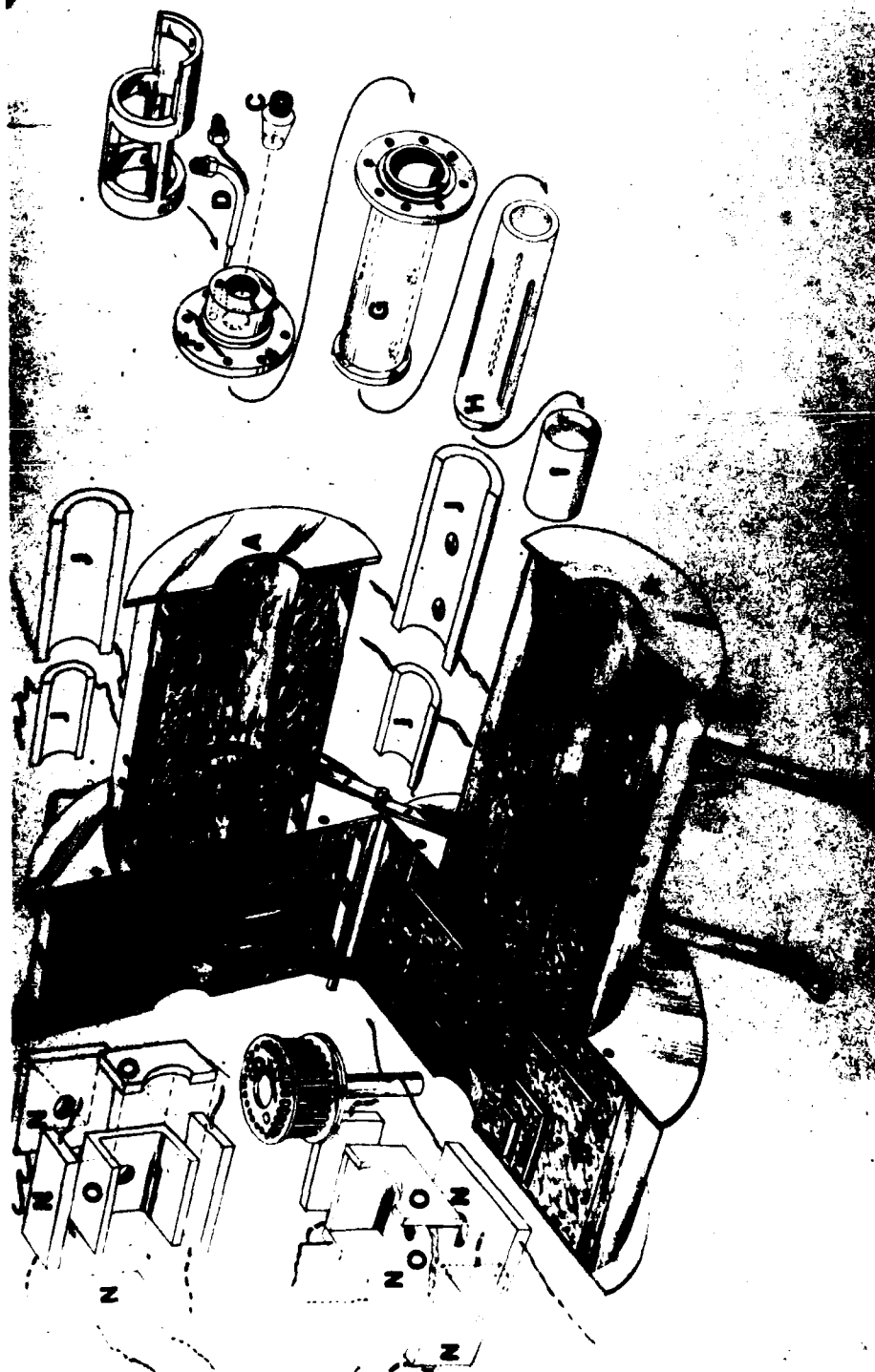


Figure 4 - Expanded View of Burner Rig Showing Placement of Essential Components

Key to Figure 4

- A. Stainless Steel Furnace Shell
- B. Refractory Cement
- C. Fuel Nozzle
- D. Sea Salt Atomizer Nozzle
- E. Support Bracket for Salt and Fuel Nozzles
- F. Alignment Tube Flange
- G. Stainless Steel Alignment Tube
- H. Slotted Ceramic Combustion Tube
- I. Combustion Tube Extension
- J. Combustion Zone Heaters
- K. On-Off Control Thermocouple Well
- L. Air Inlet
- M. Combustion Zone Control Thermocouple Well
- N. Test Chamber Heaters
- O. Test Chamber Muffles
- P. Specimen and Fixture

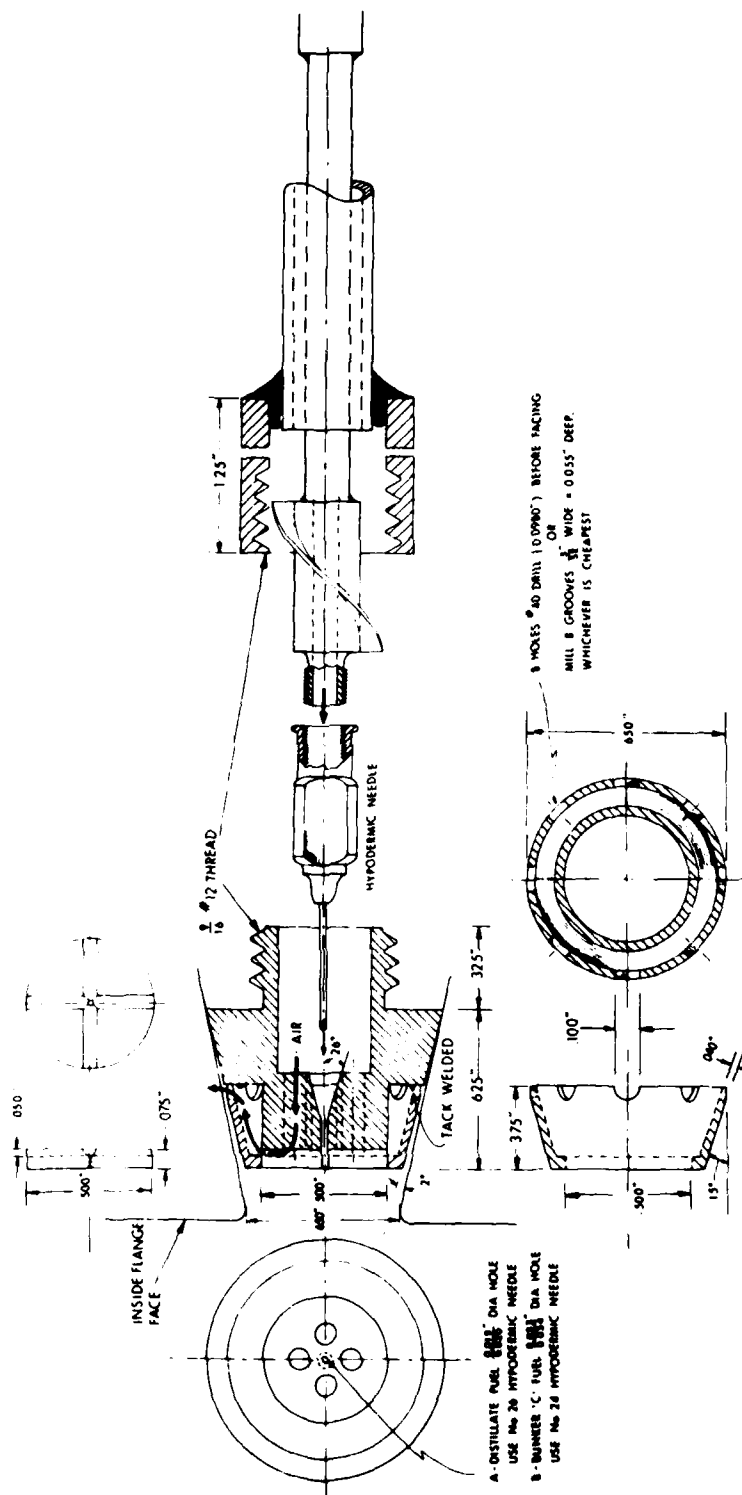


Figure 5  
Fuel Nozzle Assembly

NAVAL SHIP RESEARCH AND DEVELOPMENT LABORATORY

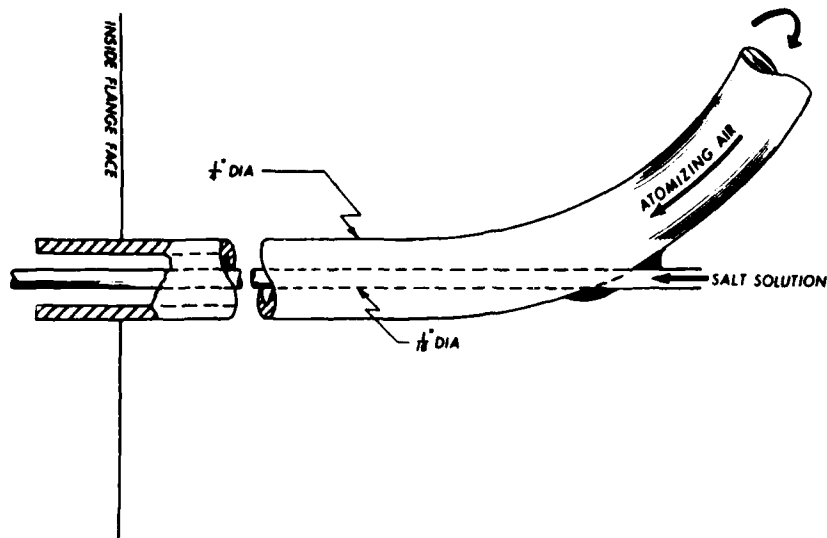


Figure 6  
Sea-Water Atomizer

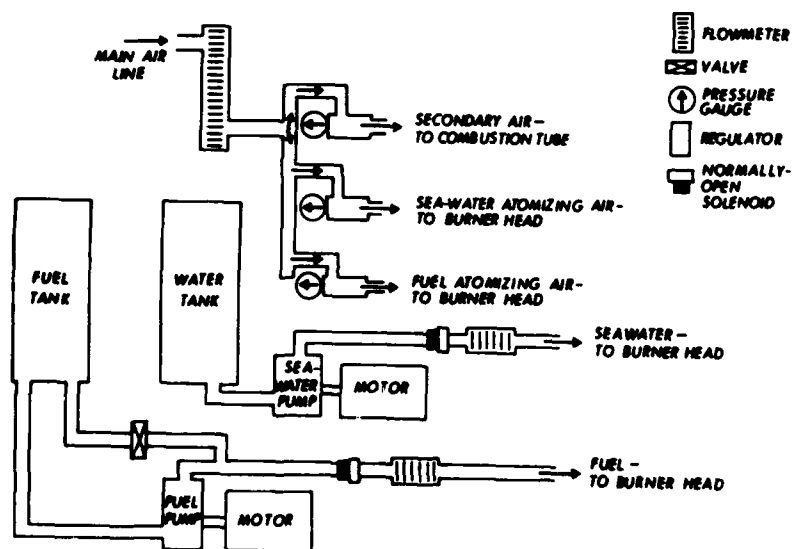


Figure 7  
Schematic Diagram of Plumbing for Fuel, Sea-Water Solution, and Air

# NAVAL SHIP RESEARCH AND DEVELOPMENT LABORATORY

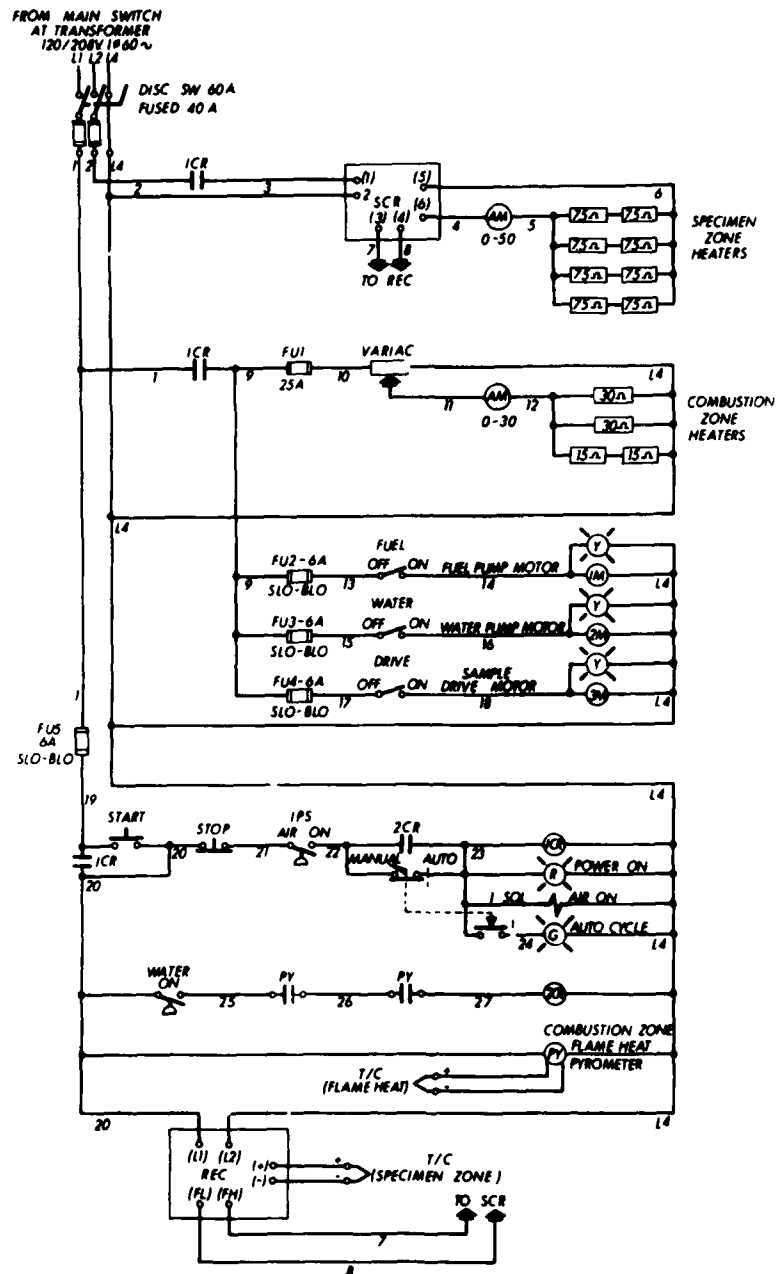


Figure 8  
Electric Circuit Diagram

NAVAL SHIP RESEARCH AND DEVELOPMENT LABORATORY

$A$  = Original Diameter, Measured With a Micrometer.

$A_1$  = Diameter of Structurally Useful Metal. Measured at 100X.

$A_2$  = Diameter of Metal Unaffected by Oxides and Sulfides.  
Measured at 100X.

SURFACE LOSS:  $A - A_1$  Loss in Diameter Due to Massive Oxides and Sulfides.

MAXIMUM ATTACK:  $A - A_2$  Loss in Diameter Due to All Forms of Oxidation and Sulfidation.

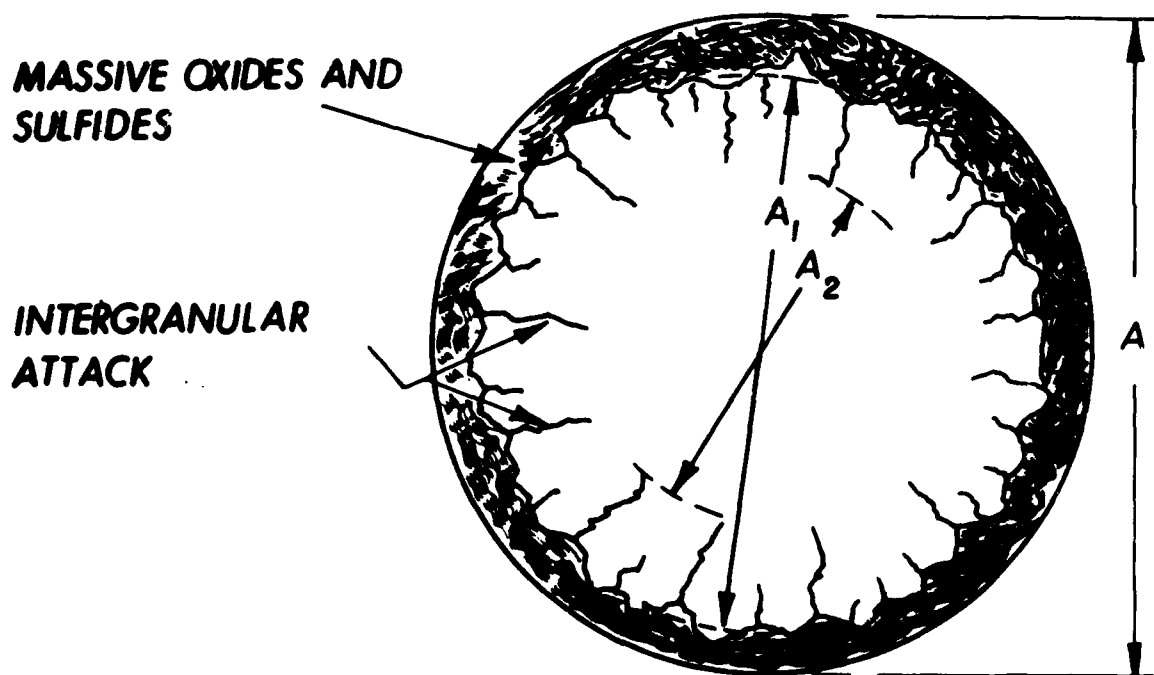


Figure 9  
Method of Measuring Hot-Corrosion Attack

NAVAL SHIP RESEARCH AND DEVELOPMENT LABORATORY

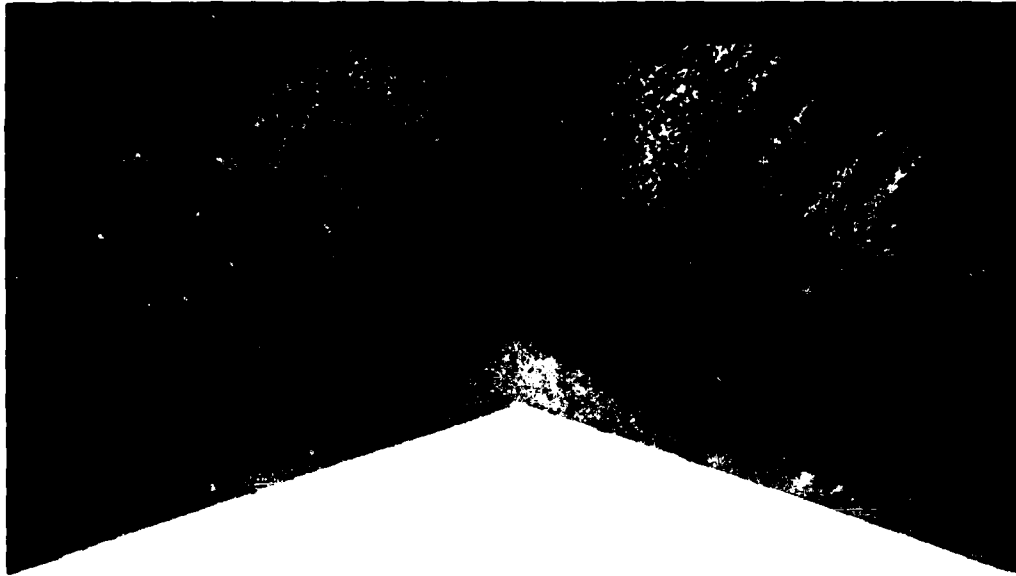


Figure 10 - Photomicrograph of Cross-Section Area of the Leading Edge of a Corroded AMS5391A Nozzle Vane (Unetched, 60X)

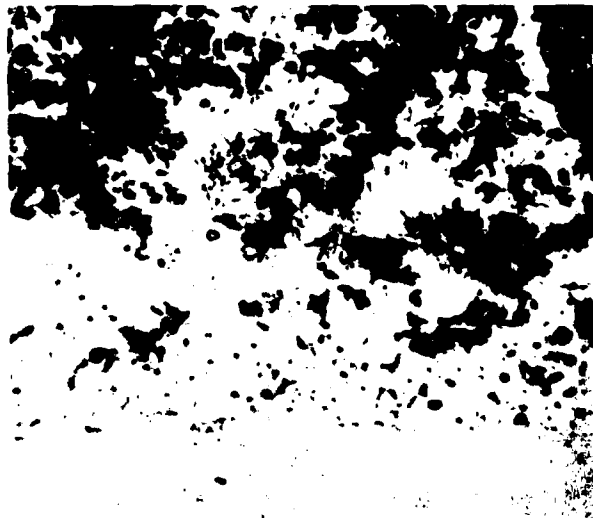


Figure 11 - Photomicrograph of the AMS5391A Nozzle Vane Illustrating the Small Grey Globular Phase at the Interface of the Oxides and Base Matrix (Unetched, 1000X)

NAVAL SHIP RESEARCH AND DEVELOPMENT LABORATORY



Figure 12 - Photomicrograph of Cross-Section Area of an  
AMS5391A Specimen Tested at 1550° F for 1000 Hours  
With 0.5 PPM Sea Salt (Unetched, 50X)

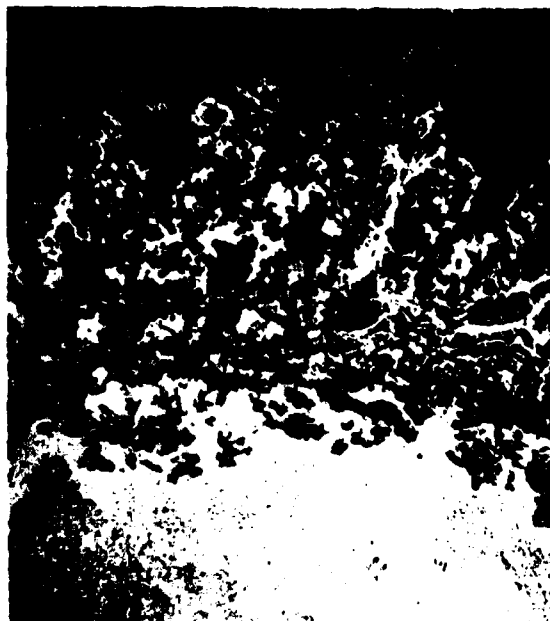
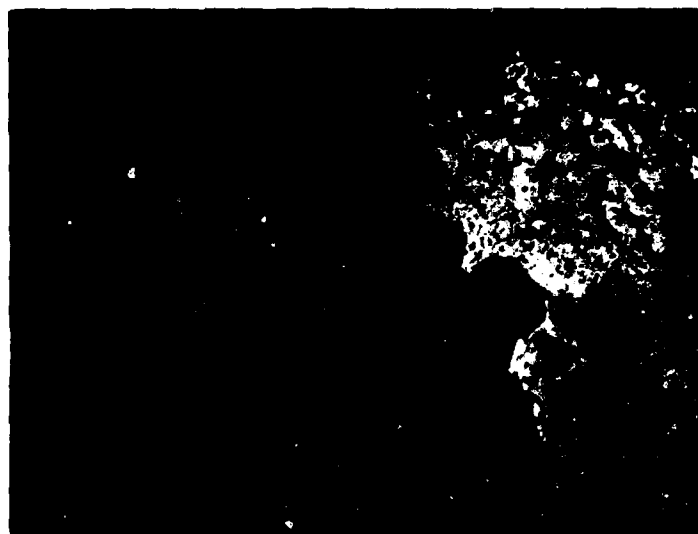


Figure 13 - Photomicrograph of Cross-Section Area of an  
AMS5391A Specimen Tested at 1600° F for 1000 Hours  
With 5 PPM Sea Salt (Unetched, 80X)

NAVAL SHIP RESEARCH AND DEVELOPMENT LABORATORY

Large Grey Chromium-Rich Sulfides (100X)



Nickel-Rich Sulfide (320X)



Figure 14 - Typical Photomicrographs of Specimen Tested  
at High Sea-Salt Concentrations  
(Marbles Reagent)

NAVAL SHIP RESEARCH AND DEVELOPMENT LABORATORY

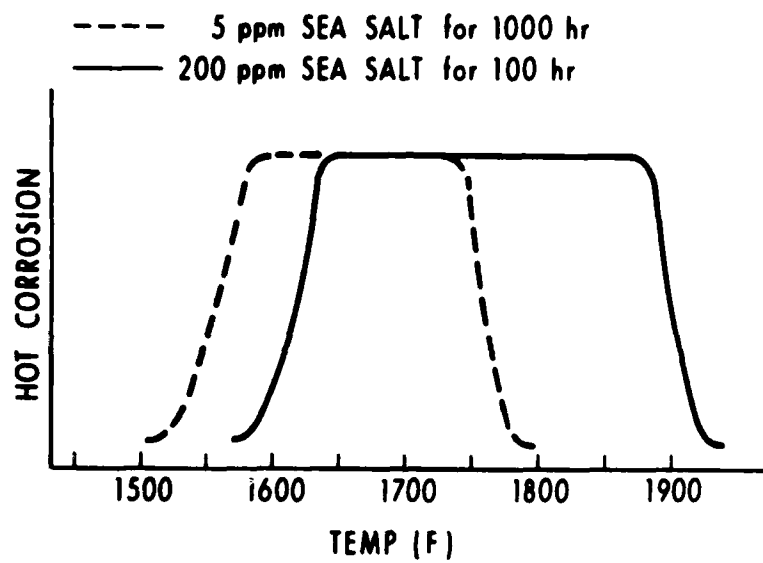


Figure 15

Temperature Range of Hot Corrosion For Two Test Conditions

## Appendix A

### Technical References

- 1 - Danek, G. J., "State-of-the-Art Survey on Hot Corrosion in Marine Gas Turbine Engines," Naval Engineer's Journal, Dec 1965, p. 859
- 2 - "Hot Corrosion Problems Associated with Gas Turbines," from Symposium at Sixty-ninth Annual Meeting ASTM, Atlantic City, 26 June - 1 July 1966, ASTM Special Technical Publication 421, Sep 1967
- 3 - Bergman, P. A., "Hot Corrosion of Gas Turbine Alloys," Corrosion, Vol. 23, No. 3, Mar 1967, p. 72
- 4 - Walters, J. J., "Study of the Hot Corrosion of Superalloys," Final Technical Report under Air Force Contract AF33(615)-5212 with AVCO/Lycoming Division, Rept AFML-TR-67-297, AD-822-779, Sep 1967
- 5 - DeCrescente, M. A., and N. S. Bornstein, "Thermodynamics of the Formation of and Reactivity of Sodium Sulfate with Gas Turbine Superalloys," from Proceedings of the Air Force Materials Laboratory Fiftieth Anniversary Technical Conference on Corrosion, at Military and Aerospace Equipment, Denver, Colorado, 23-25 May 1967, AFML-TR-67-329, Nov 1967, p. 1497

Security Classification

UNCLASSIFIED

## DOCUMENT CONTROL DATA - R &amp; D

(Security classification of title, body of abstract and indexing annotation must be entered when the overall report is classified)

1. ORIGINATING ACTIVITY (Corporate author) Naval Ship Research and Development Laboratory, Annapolis, Maryland 21402		2a. REPORT SECURITY CLASSIFICATION UNCLASSIFIED	
		2b. GROUP	
3. REPORT TITLE Construction and Operation of a Hot-Corrosion Test Facility			
4. DESCRIPTIVE NOTES (Type of report and inclusive dates) Research and Development			
5. AUTHOR(S) (First name, middle initial, last name) Harvey von E. Doering and Paul A. Bergman			
6. REPORT DATE March 1969		7a. TOTAL NO. OF PAGES 33	7b. NO. OF REFS 5
8a. CONTRACT OR GRANT NO.		9a. ORIGINATOR'S REPORT NUMBER(S) 2844	
b. PROJECT NO. SF013 06/04			
c. Task 12725 Assigt -1815-122-A		9b. OTHER REPORT NO(S) (Any other numbers that may be assigned this report) MATLAB 281	
10. DISTRIBUTION STATEMENT This document has been approved for public release and sale; its distribution is unlimited.			
11. SUPPLEMENTARY NOTES		12. SPONSORING MILITARY ACTIVITY NAVSEC (SEC 6140)	
13. ABSTRACT An apparatus, the burner rig, used to evaluate materials for use in gas-turbine engines operating in a marine environment, is described. Testing procedures are outlined, and results are discussed in relation to gas-turbine engine tests. The rig operates by the combustion of diesel oil or jet fuels. Injected seawater and the products of combustion pass over as many as 48 test specimens. Although the rig operates at atmospheric pressure and low velocities, it can generate a test environment that results in hot corrosion as found in actual engines, is economical to construct, and can operate unattended for long periods of time over a wide range of closely controlled conditions. Data are shown for some commercial nickel-and cobalt-base alloys tested at 200 parts per million (ppm) sea salt/100 hours and 5 ppm sea salt/1000 hours. Comparisons are made between photomicrographs of the corroded zones of engine parts and specimens tested at 0.5, 5.0, and 200 ppm sea salt. Empirically, 200 ppm sea salt is too heavily oriented toward sulfidizing effects, and oxidation does not play a dominant enough role in the net corrosion process. It appears that 1000 hours with 0.5 ppm sea salt represent realistic test conditions.  (authors)			

DD FORM 1473

(PAGE 1)

UNCLASSIFIED

5/N 0101-807-6801

Security Classification

**UNCLASSIFIED**

DD FORM 1473 (BACK)  
(PAGE 2)

**Security Classification**